PHOTOSYNTHETICA
International Journal for Photosynthesis Research

DOI 10.32615/ps.2023.032 PHOTOSYNTHETICA 61 (SI): 425-431, 2023

Special issue in honor of Prof. Győző Garab

Influence of reduced amounts of sulfoquinovosyl diacylglycerol on the thylakoid membranes of the diatom *Thalassiosira pseudonana*

T. LIEBISCH, M. BAŞOGLU, S. JÄGER, and C. BÜCHEL+

Institute of Molecular Biosciences, Goethe University Frankfurt, Frankfurt, Germany

Abstract

Diatom thylakoids contain much higher amounts of sulfoquinovosyl diacylglycerol (SQDG) than vascular plants and the hypothesis was brought forward that this relates to their special thylakoid structure. To test this hypothesis we created knock-down mutants in *Thalassiosira pseudonana* that exhibited a decreased SQDG content per cell. Surprisingly, the ratio between the different lipid classes did not change, pointing to strict regulation of thylakoid lipid composition. The antenna proteins, fucoxanthin–chlorophyll proteins (FCP), were reduced and photosystem (PS) I compared to PSII was increased as judged from absorbance spectra. CD spectroscopy indicated a tighter packing of chromophores. The reduction in FCP might help to avoid diametral changes in excitation energy transfer. In contrast, the increase in PSI in the mutants might counteract the diminishment of the usually huge PSI antenna. No changes in thylakoid structure were observed since the stoichiometry between different lipid classes seems to be carefully balanced.

Keywords: algae; lipids; photosynthesis; sulfoquinovosyl diacylglycerol.

Introduction

Thylakoid membrane lipids consist mainly of glycolipids, like monogalactosyl diacylglycerol (MGDG), digalactosyl diacylglycerol (DGDG), and sulfoquinovosyl diacylglycerol (SQDG). They are accompanied by phosphatidylglycerol (PG) and, in the case of diatoms, phosphatidylcholine (PC) (Lepetit *et al.* 2010, Mizusawa and Wada 2012, Kobayashi 2016). SQDG, PC, and PG are anionic lipids, which introduce charges to the membranes. In higher plants and some algae, SQGD can partially compensate for PG (Benning *et al.* 1993), and it was hypothesised that this is a mechanism to ensure the maintenance of a proper balance of anionic charges (Benning *et al.* 1993, Yu and Benning 2003) in the thylakoids.

In contrast to higher plants, diatoms contain an unusually high content of SQDG (Vieler *et al.* 2007,

Highlights

- Reducing the amount of SQDG in diatoms reduces the other lipid classes in parallel
- Enhanced chlorophyll content leads to tighter packing of pigments in the mutants
- This is balanced by a reduced FCP content and a changed PSII/PSI ratio

Received 30 May 2023
Accepted 21 August 2023
Published online 5 September 2023

+Corresponding author
e-mail: c.buechel@bio.uni-frankfurt.de

Abbreviations: CD – circular dichroism; DGDG – digalactosyl diacylglycerol; FCP – fucoxanthin–chlorophyll proteins; HL – high light; LL – low light; PC – phosphatidylcholine; PG – phosphatidylglycerol; MGDG – monogalactosyl diacylglycerol; SQD1 – UDP-sulfoquinovose synthase; SQDG – sulfoquinovosyl diacylglycerol; TLC – thin layer chromatography.

Acknowledgements: We kindly acknowledge the opportunity to use the CD spectrometer of Prof. Dr. Werner Kühlbrandt's group (MPI Biophysics, Frankfurt) and thank Martin Centola for his assistance. We are grateful for the support by Kerstin Pieper and Katharina Kuhlmeier concerning cultures, cell counting, and Chl determination and acknowledge the contribution of Nadine Zucchetto and Felix Graf to the cloning approaches and TLC method evaluation, respectively.

Conflict of interest: The authors declare that they have no conflict of interest.

Lepetit *et al.* 2012). SQDG accounts for around 25–40% in *Phaeodactylum tricornutum* and *Cyclotella meneghiniana*, the latter species being closely related to *Thalassiosira pseudonana*. In addition, the phosphatidyl-containing lipids make up about 22–26%, depending on species and light acclimation (Lepetit *et al.* 2012). The high content of negatively charged lipids has also been linked to the stacking behaviour of thylakoid membranes, since the lipid situation in diatoms resembles the lipid content of cyanobacterial photosynthetic membranes, which do not possess grana stacks in their thylakoid structure (Vieler *et al.* 2007). In diatoms, thylakoids are organized in bands of three thylakoids each, *i.e.*, six membranes, but whether these are strongly appressed comparable to the granal thylakoid membranes has not been elucidated in detail yet (Ünnep *et al.* 2014, Flori *et al.* 2017). Enrichment of PSII on the inner four membranes was reported (Flori *et al.* 2017), whereas PSI is located mainly on the outer membranes (Pyszniak and Gibbs 1992). Nonetheless, segregation is far less strict than in grana-containing organisms.

During high light (HL) acclimation, the lipid composition in diatoms changes, with an increase in SQDG at the expense of mainly MGDG (Lepetit *et al.* 2012). Together with the fact that the direct environment of light-harvesting complexes (called fucoxanthin–chlorophyll complexes, FCP, in diatoms) is enriched in MGDG, Lepetit *et al*. (2012) proposed the following hypothesis: under low light (LL), the outer membranes of a thylakoid band are enriched in SQDG and contain mainly PSI, but also small amounts of PSII with their FCPs, albeit in lower amounts compared to the four inner membranes. These are enriched in MGDG and also contain the majority of FCP complexes. The MGDG shell of the FCPs also serves as a reservoir for diadinoxanthin, which, under HL conditions, is converted to diatoxanthin (Goss *et al.* 2007). During HL adaptation, the areas of additional SQDG reach into the margin regions and maybe even into the four inner membranes. Several further lines of evidence support this hypothesis, *e.g.*, the fact that ATP-synthase, which has to be located in the outer membranes, prefers SQDG as surrounding (Pick *et al.* 1985). In addition, the negative charge of SQDG might hinder an association of the thylakoid bands.

The SQDG biosynthesis pathway was first discovered in *Rhodobacter sphaeroides* (Benning and Somerville 1992). In higher plants and algae, the sulfoquinovose head group is synthesised by the UDP-sulfoquinovose synthase (SQD1), catalysing the transformation of UDP-glucose to UDP-6-sulfoquinovose using sulfite and NAD^+. In *Arabidopsis thaliana*, SQD1 is a soluble protein, which is localised in the chloroplast stroma and whose mRNA expression level is increased under phosphate-deplete conditions (Essigmann *et al.* 1998). In 1999, the structure of the plant protein was solved by X-ray diffraction including the substrates UDP-glucose and sulfite, as well as the co-factor NAD^+ (Mulichak *et al.* 1999).

The final step of SQDG biosynthesis in plants is catalysed by the enzyme sulfoquinovosyl diacylglycerol synthase (also called SQD2), transferring the sulfoquinovosyl headgroup onto diacylglycerol (Yu *et al.* 2002).

Since SQDG is the dominant lipid class in the thylakoid membranes of diatoms besides MGDG and is hypothesised to have a role in PS segregation and thylakoid band patterning, we examined the influence of a reduced SQDG content on *T. pseudonana* cells. To this end, we created knock-down mutants where the expression of the *sqd1* gene, coding for the putative SQD1 of *T. pseudonana*, was reduced.

Materials and methods

Growth conditions: *Thalassiosira pseudonana* (CCMP1335) WT and mutants were grown in F/2 medium (Guillard 1975) under constant shaking for 7 d under 40 mmol(quanta) m^{-2} s^{-1} with a 16-h light/8-h dark cycle. For experiments including mutants, cells were grown in the same medium supplemented with 100 µg mL^{-1} *Nourseothricin* (*Werner Bioagents*).

Cloning and transformation: The *sqd1* gene of *T. pseudonana* was identified by *BLAST* search in the *Jgi* database (https://mycocosm.jgi.doe.gov/Thaps3/Thaps3.home.html) using the *A. thaliana sqd1* gene. The *Blast* search yielded a hit already annotated as 'sulfolipid biosynthesis protein' that was predicted to have a signal peptide and chloroplast transit peptide using the programs *SignalP* and *ChloroP*, respectively. It was chosen for further work (for further reasons, *see* 'Results'). Protein ID269393 has a coding sequence of 1,389 bp and one intron of 680 bp. RNA was isolated from *T. pseudonana* using Trizol/chloroform in the first step, followed by *RNeasy Mini Kit* (*Qiagen*). cDNA was generated using the *RevertAid First Strand cDNA Synthesis Kit* (*ThermoFisher Scientific*). The *sqd1* gene was amplified from cDNA by PCR using primers B_SQD1_fw and D_SQD1_rev and ligated into the pJET vector. *E. coli* XL-1 was transformed with the plasmid, and the sequence was verified. The antisense fragment was amplified from the plasmid using the primer pair L_knockdown_sqd1_fwd_SalI and M_knockdown_sqd1_rev_HindIII, and the PCR product was purified by agarose gel electrophoresis. After elution, the fragment was ligated with the vector pSKII that had been pre-linearized using EcoRV. The ligation product was used to transform *E. coli* XL1, and isolated plasmids from positive clones were digested using SalI and HindIII. The respective fragments representing the antisense sequence were ligated into pTpNR+nat, yielding the plasmids for the transformation of *T. pseudonana* that were sequenced for verification. WT cells were transformed by biolistic transformation according to Apt *et al.* (1996). The resulting clones were verified by PCR using the primers L_knockdown_sqd1_fwd_SalI and Seq_Tp_NRpro_fw. The primers used in this study are listed in the text table.

Characterisation of mutants: To quantify the success of the transformation with antisense RNA, RNA was isolated from *T. pseudonana* as described above. mRNA levels of the *sqd1* gene were determined by duplex PCR using the *actin* gene as an internal standard and the primers

Name	Sequence	Use
B_SQD1_fw	ATGAAGCTCCTCCTCCTCCTAACC	amplification *sqd1* from cDNA
D_SQD1_rev	TTAATCGGCCTTGATCTTGATGC	amplification *sqd1* from cDNA
L_knockdown _sqd1_ fwd_SalI	GTCGACTTATCCTCGGAGCCGATGG	amplification antisense fragment, verification of final plasmid
M_knockdown_sqd1_ rev_HindIII	AAGCTTGGCGAAGTGTACGATGG	amplification antisense fragment
N_knockdown_sqd1_ fwd_SalI	GTCGACTCTTCACCCTGCGTACC	amplification of *sqd1* fragment in duplex PCR
O_knockdown_sqd1_ rev_HindIII	AAGCTTCCTCCGGTTCCGTAGAC	amplification of *sqd1* fragment in duplex PCR
Seq_Tp_NRpro_fw	CTTTTCGGCAAGCACAGAGC	verification of final plasmid
Tp_act1_fw	GATATCGCTGCCCTTGTCAT	amplification of *actin* fragment in duplex PCR
Tp_act1_rev	TCCGACGTAAGCGTCTCTTT	amplification of *actin* fragment in duplex PCR

N_knockdown_sqd1_fwd_SalI, O_knockdown_sqd1_rev_HindIII, Tp_act1_fw, and Tp_act1_rev. The intensity of the bands on gels was quantified using *ImageJ*. The ratio *sqd1*/*actin* was set to 1 for WT cells. According to the mRNA results, the clones TpASsqd1-ma3s (called ma3s from now on) and TpASsqd1-ma4s (ma4s) showed the highest suppression levels and were analysed further.

Cells were counted using a Neubauer chamber, and the Chl concentration of cells was estimated spectroscopically after breakage of the cells using a tissue lyser in 90% acetone, 1 mM Tris pH 7.5, according to Jeffrey and Humphrey (1975).

Lipid extraction followed the protocol of Barka *et al.* (2016), whereby equal amounts of cells from the different clones were used as starting material. Different lipid classes were quantified using thin layer chromatography (TLC) according to Lepetit *et al.* (2010), except that for the second run a mixture of hexane:diethylether:acetic acid (70:30:2, v:v:v) was used. Dilution series of the extracts were applied to the TLC plates. Analysis was done using *ImageJ* to determine spot intensities, and regression lines for each of the dilution series were calculated to determine the ratio of SGDG content in WT and mutants. *ImageJ* was also used to determine the relative quantity of MGDG, DGDG, SQDG, PC, and PG in WT and mutants. An example of a TLC plate is shown in Fig. 1S (*supplement*). The identity of the lipids was confirmed using standards at 1.5 µg per lane, purchased from *Larodan* (Sweden). By using the Chl *a*/cell ratio determined before, a comparison based on cell number or Chl concentration could be made.

Circular dichroism (CD) spectra of WT and mutant cells were recorded from 350 to 750 nm with a *Jasco J-810* dichrograph (sensitivity: 100 mdeg; optical path length: 1 cm), which was equipped with a *Jasco PTC-423S* Peltier element. Measurements were carried out at room temperature (22°C), using a 3-nm bandpass, a scanning speed of 50 nm min^{-1}, and a response time of 8 s. Great care was taken to adjust cells to a comparable optical density in the Q_Y absorption band of around 0.6. Absorbance spectra were recorded in parallel. All spectra were taken from at least three independent cultures of WT and mutants each.

For electron microscopy, cells were fixed in 2.5 % (v/v) glutaraldehyde in a growth medium for 1 h at 4°C and then washed twice with sodium cacodylate buffer (0.05 M Na-cacodylate, 0.4 M sucrose, pH 7.2), before they were treated with 2% (w/v) osmium tetroxide. Dehydration was done with a series of increasing ethanol concentrations. Afterward, cells were embedded in araldite and cut into ultra-thin sections using a diamond knife. Sections were treated with uranyl acetate and lead citrate to enhance the contrast and were then examined in a *Philips CM12* TEM. Distances between thylakoid bands were measured using *ImageJ*. Thirty measurements per strain were carried out for six different cells each. Great care was taken to only examine and analyse thylakoid bands that were running strictly parallel.

Statistical analysis: Where applicable, values are expressed as means and standard deviations, whereby the number of independent measurements is given in the figure legends. *T*-tests were applied to test for statistical significance.

Results

To characterize the effect of SQDG in the thylakoid membrane of the diatom *T. pseudonana*, we wanted to generate antisense mutants for one of the enzymes of the biosynthesis pathway, the UDP-sulfoquinovose synthase (SQD1). To identify the *sqd1* gene in *T. pseudonana*, the *A. thaliana* SQD1 protein sequence was used in a *BLAST* search against the translated *T. pseudonana* genome. This search revealed a sensible hit (JGI ID269393) with a total query cover of 84%, already annotated as 'sulfolipid biosynthesis protein'. This sulfolipid biosynthesis protein had a signal peptide and a plastidic target protein sequence prediction in accordance with a putative localisation in the plastid. In agreement with the high sequence identity, the active centre of SQD1, the NAD^+ pyrophosphate-binding site, and the UDP-glucose-binding site were present. Remarkably, a *P. tricornutum* protein was identified, which was fairly similar to the *T. pseudonana* candidate (JGI ID21201, identity 78%). This underlined the high probability of this candidate representing the *sqd1* of diatoms. Moreover, the diatom *EST* database suggested that its mRNA was expressed under different environmental conditions.

Sqd1 was indeed expressed in WT, as shown in Fig. 1*A*. We then generated antisense mutants by targeting the sequence section of the putative NAD^+ pyrophosphate-binding site of *sqd1*. After transformation and selection,

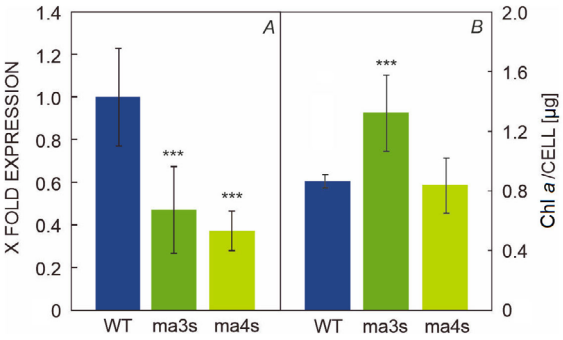

Fig. 1. Basic characterisation of *sqd1*-mutants. mRNA was quantified using duplex PCR with *actin* as a housekeeping gene for normalisation (*A*). Values represent means and standard deviations of three independent RNA isolations. In (*B*) the Chl content in µg per cell is given. Values in (*B*) represent the means and standard deviations of two biological replicates tested in triplicate. *** denotes a significant difference to WT with $p<0.005$.

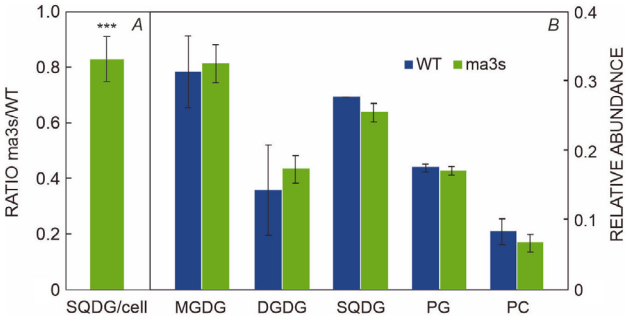

Fig. 2. Lipid composition in WT and mutant line ma3s. Lipids were quantified using TLC, and the ratio of the amount of SQDG in ma3s and WT per cell was calculated (*A*). In (*B*), the same TLCs were used to analyse the relative distribution of PC, PG, SQDG, DGDG, and MGDG in ma3s and WT, whereby the sum of the lipids classes analysed was set to 1. The values represent the means and standard deviations of two independent lipid extractions tested in triplicates. *** in (*A*) denotes significantly different to WT with $p<0.001$; in (*B*) differences between WT and ma3s are not significant.

positive clones were tested for their relative expression levels of *sqd1*. Strains ma3s and ma4s showed the best results with about 50 or 40% expression remaining, respectively (Fig. 1*A*).

Mutant line ma3s grew slower (Fig. 2S, *supplement*) but showed a significantly increased Chl/cell ratio, which was enhanced by a factor of around 1.5 compared to WT (Fig. 1*B*). Changes in ma4s were much smaller and not significant. We thus focussed on ma3s for the following experiments. Additional data on ma4s can be found in Figs. 2S–4S (*supplement*).

Reduced mRNA levels do not necessarily translate to a reduced amount of protein or decreased amounts of products of enzymatic action. Since no antibody was available, we directly checked for the amount of SQDG present in mutant and WT.

As shown in Fig 2*A*, the mutant ma3s showed a reduced SQDG content per cell in comparison to WT by about 20%, although the suppression of transcription of *sqd1* was 60%. Since ma3s showed an increased content of Chl per cell, the reduction in SQDG per Chl was even higher, with a remaining SQDG level of 50% in the mutants compared to WT. The ratio of the various lipid groups, however, did not change significantly between mutant and WT (Fig. 2*B*).

SQDG is one of the major lipid classes in the thylakoid membrane, and thus a change in thylakoid structure might be induced by lowering its amount despite the unchanged ratio to other lipid classes. To test this hypothesis, we examined the cells using thin-section electron microscopy. The typical arrangement of thylakoids in bands of six membranes (three thylakoids) each was preserved in the mutants (Fig. 3). On the other hand, ma3s exhibited fewer bands per chloroplast, *i.e.*, the gap between different stacks of three was larger in the mutants, although the distance between single thylakoid membranes seemed unaltered. We analysed this further by measuring

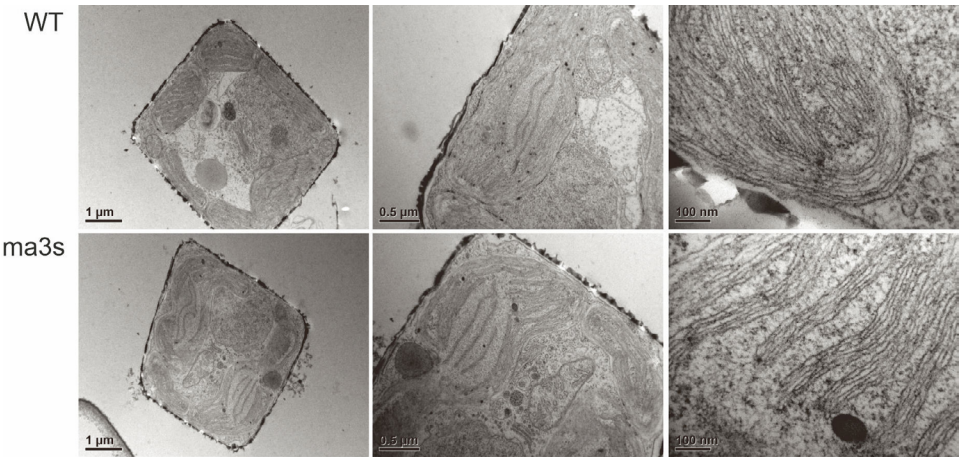

Fig. 3. Transmission electron microscopy pictures of *Thalassiosira pseudonana* WT and the ma3s mutant. Pictures in the left panel were acquired at a magnification of 11,500×, whereas the images in the middle and right panel correspond to magnifications of 25,000× and 53,000×, respectively.

the distance between thylakoid bands in WT and mutant cells. WT thylakoid bands were 28.78 ± 11.94 nm apart, whereas this value was increased to 59.39 ± 15.08 nm in ma3s (n = 30, p<0.001). The size of the cells and chloroplasts, as well as the number of chloroplasts, was not changed. Thus, the reduced amount of lipids per cell translated to fewer thylakoid bands per chloroplast.

To investigate the phenotype of the mutant in more detail, absorbance and CD spectra of whole cells were recorded at room temperature. Fig. 4*A–C* demonstrates the differences in the absorbance between WT and ma3s. WT has a much higher absorbance between 350 nm and 550 nm, *i.e.*, in the Soret region of Chl and carotenoid absorbance (Fig. 3*A*,*C*). On the other hand, the Q_Y maximum of Chl *a* is shifted to a longer wavelength in the mutant, from 677 nm in WT to 678.5 nm in ma3s (Fig. 4*B*,*C*). The changes in absorbance are accompanied by changes in the CD spectra (Fig. 4*D*). The slight reduction in carotenoids became again visible in the spectra of ma3s. However, the changes in the long wavelength bands were much more prominent, with an increase especially in the (+)694 nm but also in the (–)675 nm band. In ma3s, the former was increased by a factor of 2.17 ± 0.19 (n = 3, p<0.001) compared to WT and by 1.34 ± 0.14 nm (n = 3, p<0.05) for the negative band. The small deviations seen in the wavelength region where carotenoids absorb were not significant.

Discussion

The putative gene for the first step in the synthesis of SQDG had only been annotated as 'sulfolipid biosynthesis protein' in the *JGI* database so far, and no proof existed whether it codes for a UDP-sulfoquinovose synthase. Here, we used an antisense approach to downregulate its expression, by targeting the part of the sequence coding for the potential NAD^+ pyrophosphate-binding site of the protein. Clones having expression levels of around 50% of that of WT indeed showed a reduction in the amount of SQDG per cell. Thus, we were able to confirm protein ID269393 as SQD1, an enzyme involved in the synthesis of SQDG in diatoms.

The remaining levels of SQDG per cell were 80%, and most importantly, the ratio between the different lipid classes did not change significantly, implying that the amount of other lipids became reduced to about the same extent. In addition, mutants had an increased content of Chl. Thus, the ratio of SQDG per Chl was even smaller in the mutants compared to WT. Together with the fact of an unchanged pattern of lipid classes, this can only be explained if the density of Chl, and thus the pigment–protein complexes, were higher in the thylakoids of mutants than in WT.

In agreement with the lowered lipid concentration, the thylakoid bands in the chloroplasts of the mutant ma3s were more separated, *i.e.*, fewer bands were present per chloroplast. Since no obvious changes in cell and plastid size occurred, this relates to fewer thylakoid bands per cell. However, the structure of the bands did not change, *i.e.*, the arrangement of three thylakoids in one band, as well as the distance between single thylakoid membranes inside a band. This argues again for a denser packing of Chl inside the thylakoid membranes of ma3s.

Cells of the mutants displayed a lower absorbance in the region where carotenoids and Chls absorb. The difference spectrum (WT minus mutant, Fig. 4*C*) strongly resembles

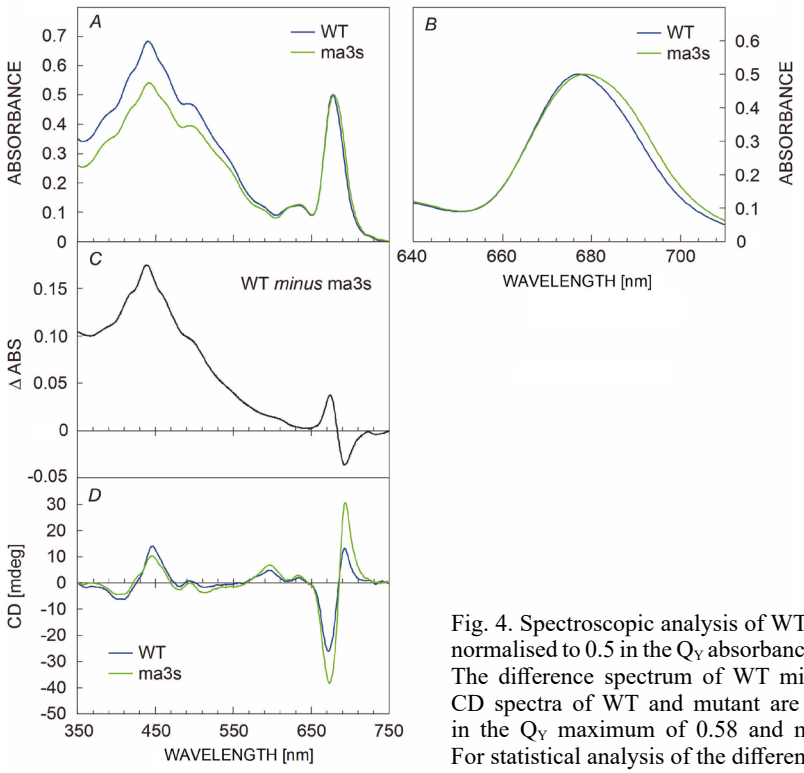

Fig. 4. Spectroscopic analysis of WT and ma3s cells. Representative absorbance spectra normalised to 0.5 in the Q_Y absorbance are shown in (*A*), with an enlargement given in (*B*). The difference spectrum of WT minus ma3s is shown in (*C*). In (*D*), representative CD spectra of WT and mutant are depicted. WT was recorded at an optical density in the Q_Y maximum of 0.58 and ma3s had an optical density of 0.56, respectively. For statistical analysis of the differences *see* text.

a spectrum of FCPs (Büchel 2003), implying a decrease of FCPs to the photosystems (PS). In addition, mutants displayed their maximum Q_Y absorbance at a longer wavelength in comparison to WT. This might be related to (stress-induced) aggregation of FCPs, as hypothesised to occur during nonphotochemical quenching (Gundermann and Büchel 2012). However, the absorbance of single FCPs was demonstrated to be around 671 nm, *i.e.*, far away from the wavelength reported here. Even fluorescence emission at room temperature is not shifted much upon aggregation (Gundermann and Büchel 2012). Another more likely hypothesis is a shift due to a change in the amount of long-wavelength chlorophylls that are present in PSI. Thus, the mutants most probably contain more PSI in relation to PSII than WT.

The changes in absorbance became also visible in CD. In the short wavelength region, signals due to carotenoids were only slightly reduced in the mutants. More importantly, signals in the long-wavelength region at about (–)675 and (+)693 nm were significantly enlarged. These signals are of non-excitonic origin (Garab *et al.* 1991, Büchel and Garab 1997, Szabó *et al.* 2008, Jäger and Büchel 2019) and the positive band can be considered a psi-type band that can be used as a fingerprint for the long-range chiral order of pigments (Szabó *et al.* 2008, Nagy *et al.* 2012). Recently we were able to demonstrate that the positive band is sensitive to membrane appression as shown for other organisms before, but is also responding to disturbances in excitation energy transfer from FCPs to PSs, *i.e.*, the lateral arrangement of the pigment–protein complexes (Jäger and Büchel 2019). The short wavelength band was sensitive to the (de)stabilisation of thylakoid membranes. The fact that both bands increase in intensity can be interpreted as a denser packing of pigment–protein complexes.

What can be concluded about the effects of reducing SGDG on thylakoid structure? First of all, the ratio of lipid classes seems to be extremely important for diatoms, since a 20% reduction in SQDG did not significantly change its ratio to other lipids. In higher plants, reduction of phosphatidyl glycerol, *e.g.*, by phosphate limitation, results in an upregulation of SQDG (Benning *et al.* 1993). In *T. pseudonana*, the SQDG to PG ratio changed from about 3 to 7 when cells were transferred to a medium without phosphate (Martin *et al.* 2011). The reverse would be expected in the case of reduced SQDG, but this is not the case. However, when comparing growth under HL and LL conditions in *C. meneghiniana*, the amounts of SQDG decreased from 40% under HL to 33% of total lipids under LL (Lepetit *et al.* 2012). No lower values are reported, which gives rise to the assumption that a minimal fraction of SQDG might be crucial for the function of photosynthesis in diatoms. This might be due to the fact that in plants and green algae, but also diatoms, SQDG is closely associated with pigment–protein complexes and thus important for their function (Gounaris and Barber 1985, Sigrist *et al.* 1988). In diatoms, PSII–FCPII supercomplexes were reported to contain eight (Pi *et al.* 2019) or five molecules of SQDG (Nagao *et al.* 2022). For PSI–FCP supercomplexes none (Nagao *et al.* 2020) or two SQDG are described (Xu *et al.* 2020). According to our data, however, diatom cells seem to be able to live with a reduced thylakoid area and thus a tighter packing of PS and FCPs. This is astonishing since more densely packed pigments should influence excitation energy transfer between pigmented complexes. This might at least partly be counterbalanced by the reduced amount of FCPs per PS. On the other hand, the PSI content relative to PSII was increased in the mutants. This is not easily accommodated with the hypothesis of a localisation of PSI in the SGDG-rich outer membranes. However, in a xanthophyte using freeze fracturing, a patchier pattern for the distribution of PSs has been reported (Büchel *et al.* 1992). Thus, only ATP synthase might depend directly on SQDG, whereas PSI of the outer membrane might be found in less SQDG-rich patches thereof. PSI was reported to contain up to 22 FCP antennae in the diatom *Chaetoceros gracilis* (Nagao *et al.* 2020, Xu *et al.* 2020). If those are reduced in numbers as well, a higher amount of PSI might help the mutants to balance their electron transport under conditions of smaller PSI antennae.

In summary, the SGDG content was only slightly reduced when suppressing *sqd1* expression. Cells managed to keep the ratio between different lipid classes constant by accordingly reducing the number of other lipid classes and by decreasing the number of thylakoid bands. By this, thylakoid organisation in bands of three remained almost unchanged. In contrast, Chl content was increased, which argues for a tighter packing of pigment–protein complexes, as also visible in CD spectra. Under these conditions, the ratio between FCPs, PSII, and PSI was adapted with more PSI and fewer FCPs in the mutants.

References

Apt K.E., Grossman A.R., Kroth-Pancic P.G.: Stable nuclear transformation of the diatom *Phaeodactylum tricornutum*. – Mol. Gen. Genet. **252**: 572-579, 1996.

Barka F., Angstenberger M., Ahrendt T. *et al.*: Identification of a triacylglycerol lipase in the diatom *Phaeodactylum tricornutum*. – BBA-Mol. Cell Biol. L. **1861**: 239-248, 2016.

Benning C., Beatty J.T., Prince R.C., Somerville C.R.: The sulfolipid sulfoquinovosyldiacylglycerol is not required for photosynthetic electron transport in *Rhodobacter sphaeroides* but enhances growth under phosphate limitation. – PNAS **90**: 1561-1565, 1993.

Benning C., Somerville C.R.: Identification of an operon involved in sulfolipid biosynthesis in *Rhodobacter sphaeroides*. – J. Bacteriol. **174**: 6479-6487, 1992.

Büchel C.: Fucoxanthin-chlorophyll proteins in diatoms: 18 and 19 kDa subunits assemble into different oligomeric states. – Biochemistry **42**: 13027-13034, 2003.

Büchel C., Garab G.: Organization of the pigment molecules in the chlorophyll *a*/*c* light-harvesting complex of *Pleurochloris meiringensis* (Xanthophyceae). Characterization with circular dichroism and absorbance spectroscopy. – J. Photoch. Photobio. B **37**: 118-124, 1997.

Büchel C., Wilhelm C., Hauswirth N., Wild A.: Evidence for a lateral heterogeneity by patch-work like areas enriched in photosystem I complexes in the three thylakoid lamellae of *Pleurochloris meiringensis* (Xanthophyceae). – Crypt. Bot. **2**: 375-386, 1992.

Essigmann B., Güler S., Narang R.A. *et al.*: Phosphate availability

affects the thylakoid lipid composition and the expression of SQD1, a gene required for sulfolipid biosynthesis in *Arabidopsis thaliana*. – PNAS **95**: 1950-1955, 1998.

Flori S., Jouneau P.-H., Bailleul B. *et al.*: Plastid thylakoid architecture optimizes photosynthesis in diatoms. – Nat. Commun. **8**: 15885, 2017.

Garab G., Kieleczawa J., Sutherland J.C. *et al.*: Organization of pigment-protein complexes into macrodomains in the thylakoid membranes of wild-type and chlorophyll *b*-less mutant of barley as revealed by circular dichroism. – Photochem. Photobiol. **54**: 273-281, 1991.

Goss R., Latowski D., Grzyb J. *et al.*: Lipid dependence of diadinoxanthin solubilization and de-epoxidation in artificial membrane systems resembling the lipid composition of the natural thylakoid membrane. – BBA-Biomembranes **1768**: 67-75, 2007.

Gounaris K., Barber J.: Isolation and characterization of a photosystem II reaction centre lipoprotein complex. – FEBS Lett. **188**: 68-72, 1985.

Guillard R.R.L.: Culture of phytoplankton for feeding marine invertebrates. – In: Smith W.L., Chanley M.H. (ed.): Culture of Marine Invertebrate Animals. Pp. 29-60. Springer, Boston 1975.

Gundermann K., Büchel C.: Factors determining the fluorescence yield of fucoxanthin-chlorophyll complexes (FCP) involved in non-photochemical quenching in diatoms. – BBA-Bioenergetics **1817**: 1044-1052, 2012.

Jäger S., Büchel C.: Cation-dependent changes in the thylakoid membrane appression of the diatom *Thalassiosira pseudonana*. – BBA-Bioenergetics **1860**: 41-51, 2019.

Jeffrey S.W., Humphrey G.F.: New spectrometric equations for determining chlorophyll *a*, *b*, c_1 and c_2 in higher plants, algae and natural phytoplankton. – Biochem. Physiol. Pflanzen **167**: 191-194, 1975.

Kobayashi K.: Role of membrane glycerolipids in photosynthesis, thylakoid biogenesis and chloroplast development. – J. Plant Res. **129**: 565-580, 2016.

Lepetit B., Goss R., Jakob T., Wilhelm C.: Molecular dynamics of the diatom thylakoid membrane under different light conditions. – Photosynth. Res. **111**: 245-257, 2012.

Lepetit B., Volke D., Gilbert M. *et al.*: Evidence for the existence of one antenna-associated, lipid-dissolved and two protein-bound pools of diadinoxanthin cycle pigments in diatoms. – Plant Physiol. **154**: 1905-1920, 2010.

Martin P., van Mooy B.A.S., Heithoff A., Dyhrman S.T.: Phosphorus supply drives rapid turnover of membrane phospholipids in the diatom *Thalassiosira pseudonana*. – ISME J. **5**: 1057-1060, 2011.

Mizusawa N., Wada H.: The role of lipids in photosystem II. – BBA-Bioenergetics **1817**: 194-208, 2012.

Mulichak A.M., Theisen M.J., Essigmann B. *et al.*: Crystal structure of SQD1, an enzyme involved in the biosynthesis of the plant sulfolipid headgroup donor UDP-sulfoquinovose. – PNAS **96**: 13097-13102, 1999.

Nagao R., Kato K., Ifuku K. *et al.*: Structural basis for assembly and function of a diatom photosystem I-light-harvesting supercomplex. – Nat. Commun. **11**: 2481, 2020.

Nagao R., Kato K., Kumazawa M. *et al.*: Structural basis for different types of hetero-tetrameric light-harvesting complexes in a diatom PSII-FCPII supercomplex. – Nat. Commun. **13**: 1764, 2022.

Nagy G., Szabó M., Ünnep R. *et al.*: Modulation of the multilamellar membrane organization and of the chiral macrodomains in the diatom *Phaeodactylum tricornutum* revealed by small-angle neutron scattering and circular dichroism spectroscopy. – Photosynth. Res. **111**: 71-79, 2012.

Pi X., Zhao S., Wang W. *et al.*: The pigment-protein network of a diatom photosystem II-light-harvesting antenna supercomplex. – Science **365**: eaax4406, 2019.

Pick U., Gounaris K., Weiss M., Barber J.: Tightly bound sulpholipids in chloroplast CF_0-CF_1. – BBA-Bioenergetics **808**: 415-420, 1985.

Pyszniak A.M., Gibbs S.P.: Immunocytochemical localization of photosystem I and the fucoxanthin-chlorophyll *a*/*c* light-harvesting complex in the diatom *Phaeodactylum tricornutum*. – Protoplasma **166**: 208-217, 1992.

Sigrist M., Zwillenberg C., Giroud C. *et al.*: Sulfolipid associated with the light-harvesting complex associated with photosystem II apoproteins of *Chlamydomonas reinhardii*. – Plant Sci. **58**: 15-23, 1988.

Szabó M., Lepetit B., Goss R. *et al.*: Structurally flexible macro-organization of the pigment–protein complexes of the diatom *Phaeodactylum tricornutum*. – Photosynth. Res. **95**: 237-245, 2008.

Ünnep R., Zsiros O., Solymosi K. *et al.*: The ultrastructure and flexibility of thylakoid membranes in leaves and isolated chloroplasts as revealed by small-angle neutron scattering. – BBA-Bioenergetics **1837**: 1572-1580, 2014.

Vieler A., Wilhelm C., Goss R. *et al.*: The lipid composition of the unicellular green alga *Chlamydomonas reinhardtii* and the diatom *Cyclotella meneghiniana* investigated by MALDI-TOF MS and TLC. – Chem. Phys. Lipids **150**: 143-155, 2007.

Xu C., Pi X., Huang Y. *et al.*: Structural basis for energy transfer in a huge diatom PSI-FCPI supercomplex. – Nat. Commun. **11**: 5081, 2020.

Yu B., Benning C.: Anionic lipids are required for chloroplast structure and function in *Arabidopsis*. – Plant J. **36**: 762-770, 2003.

Yu B., Xu C., Benning C.: *Arabidopsis* disrupted in *SQD2* encoding sulfolipid synthase is impaired in phosphate-limited growth. – PNAS **99**: 5732-5737, 2002.